

Bayesian inference with data-driven image priors

Marcelo Pereyra

Heriot-Watt University
& Maxwell Institute



Joint work with



Matthew Holden
(Maxwell Institute)



Kostas Zygalakis
(Edinburgh University
& Maxwell Institute)

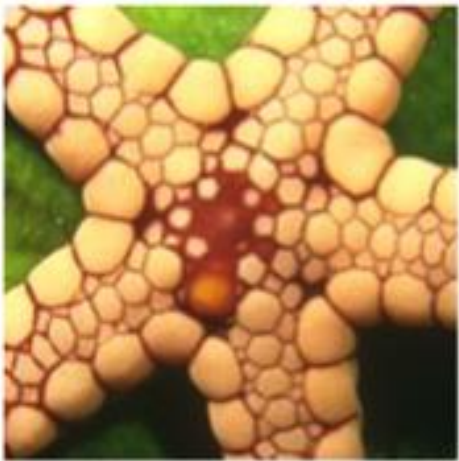


Andrés Almansa
(CNRS, University of Paris)

Outline

- **Introduction**
- Proposed method
- Experiments

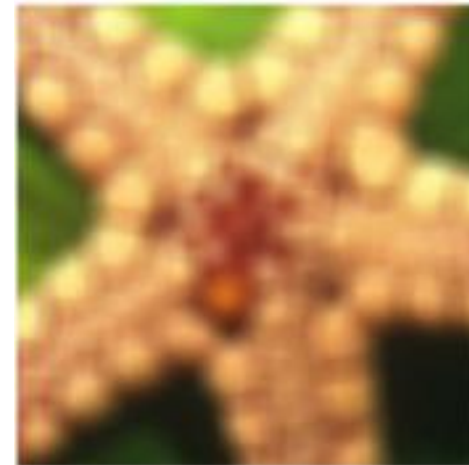
Forward problem



True scene

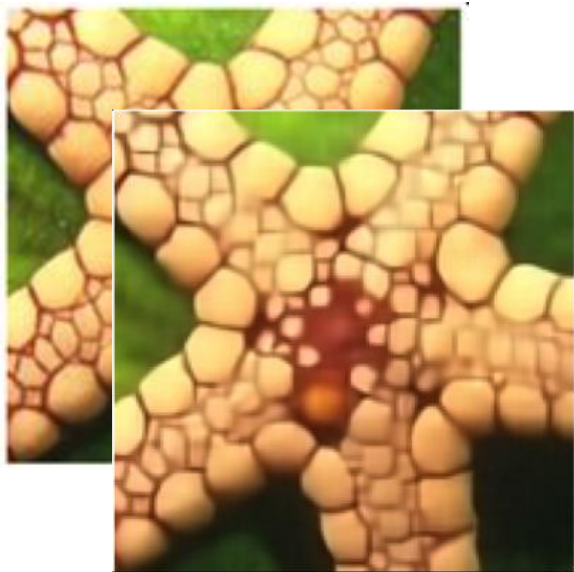


Imaging device



Observed image

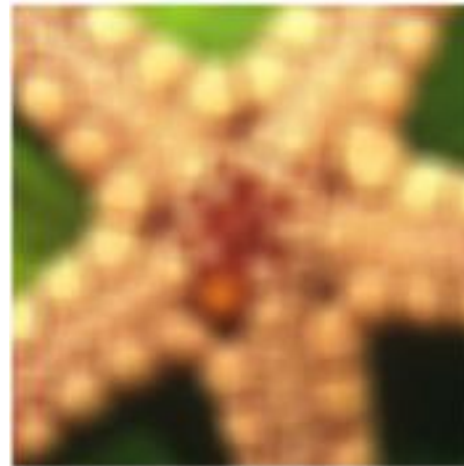
Inverse problem



Estimated scene



Imaging **method**



Observed image

Problem statement

- We are interested in recovering an unknown image $x \in \mathbb{R}^d$, e.g.,
- We measure y , related to x by some mathematical model.
- For example, many imaging problems involve models of the form

$$y = Ax + w,$$


for some linear operator A , and some perturbation or “noise” w .

- The recovery of x from y is often ill-posed or ill-conditioned, so we regularize it.

Bayesian statistics

- We formulate the estimation problem in the Bayesian statistical framework, a probabilistic mathematical framework in which we represent x as a random quantity and use probability distributions to model expected properties.
- To derive inferences about x from y we postulate a joint statistical model $p(x, y)$ typically specified via the decomposition $p(x, y) = p(y|x)p(x)$.
- The Bayesian framework is equipped with a powerful decision theory to derive solutions and inform decisions and conclusions in a rigorous and defensible way.

Bayesian statistics

- The decomposition $p(x, y) = p(y|x)p(x)$ has two ingredients:
- The **likelihood**: the conditional distribution $p(y|x)$ that models the data observation process (the forward model).
- The **prior**: the marginal distribution $p(x) = \int p(x, y) dy$ that models expected properties of the solutions.
- In imaging, $p(y|x)$ usually has significant identifiability issues and we rely strongly on $p(x)$ to regularize the estimation problem and deliver meaningful solutions.

Bayesian statistics

- We base our inferences on the **posterior** distribution

$$p(x|y) = \frac{p(x, y)}{p(y)} = \frac{p(y|x)p(x)}{p(y)}$$

where $p(y) = \int p(x, y) dx$ provides an indication of the goodness of fit.

- The conditional distribution $p(x|y)$ models our knowledge about the solution x after observing the data y , in a manner that is clear, modular and elegant.
- Inferences are then derived by using **Bayesian decision theory**.

Bayesian statistics

There are three main challenges in deploying Bayesian approaches in imaging sciences:

1. Bayesian computation: calculating probabilities and expectations w.r.t. $p(x|y)$ is computationally expensive, although algorithms are improving rapidly.
2. Bayesian analysis: we do not usually know what questions to ask $p(x|y)$, imaging sciences are a field in transition and the concept of *solution* is evolving.
3. Bayesian modelling: while it is true that *all models are wrong, but some are useful*, image models are often too simple to reliably support advanced inferences.

Outline

- Introduction
- **Proposed method**
- Experiments

In this talk

- Instead of specifying an analytic form for $p(x)$, we consider the situation where the prior knowledge about x is available as a set of examples $\{x'_i\}_{i=1}^M$ i.i.d. w.r.t x .
- We aim to combine this prior knowledge with a likelihood $p(y|x)$ specified analytically to derive a posterior distribution for $p(x|y, \{x'_i\}_{i=1}^M)$.
- The goal is to construct $p(x|y, \{x'_i\}_{i=1}^M)$ in a way that preserves the modularity and interpretability of analytic Bayesian models, and enables efficient computation.

Bayesian model

- Following the *manifold hypothesis*, we assume that x takes values close to an unknown p -dimensional submanifold of \mathbb{R}^d .
- To estimate this submanifold from $\{x'_i\}_{i=1}^M$, we introduce a latent representation $z \in \mathbb{R}^p$ with $p \ll d$, and a mapping $\phi : \mathbb{R}^p \rightarrow \mathbb{R}^d$, such that the pushforward measure under ϕ of $z \sim N(0, I_p)$ is close to the empirical distribution of $\{x'_i\}_{i=1}^M$.
- Given ϕ , the likelihood $p(y|z) = p_{y|x}(y|\phi(z))$. We can then easily derive the posterior $p(z|y) \propto p(y|z)p(z)$ and benefit from greatly reduced dimensionality.
- The posterior $p(x|y)$ is simply the pushforward measure of $z|y$ under ϕ .

Estimating ϕ

- There are different learning approaches to estimate ϕ , e.g., variational auto-encoders (VAE)s and generative adversarial networks (GAN)s.
- We use a VAE, i.e., we assume x is generated from the latent variable z as follows:

$$z \sim N(0, I_p), \quad x \sim p(x|z)$$

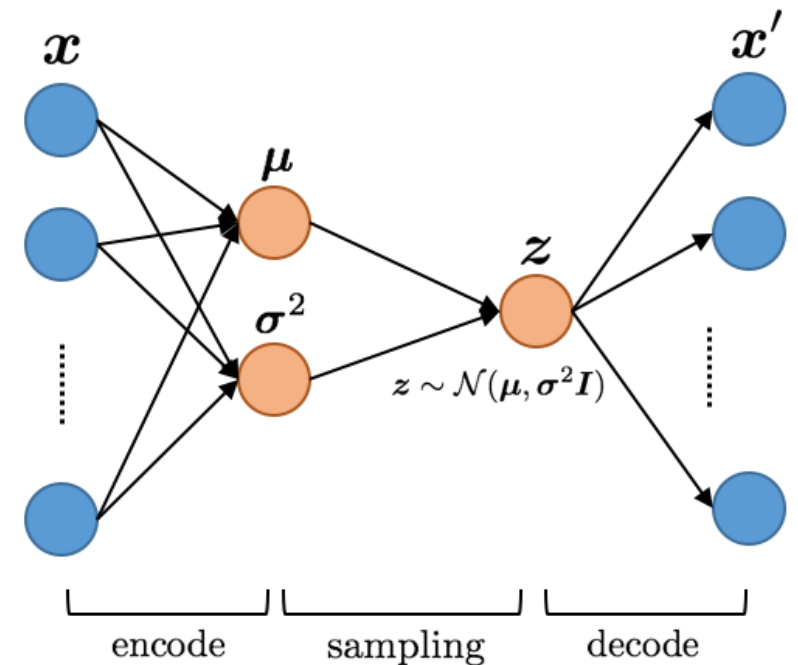
- As $p(x|z)$ is unknown, we approximate it by a parameterized distribution $p_\theta(x|z)$ defined by a neural network (**the decoder**). This typically has form $N(\mu_X(z), \sigma_X^2(z) I)$.
- The objective is to set θ to maximize the marginal likelihood $p_\theta(x'_1, \dots, x'_M)$. This is usually computationally intractable, so we maximize a lower bound instead.

Variational Auto-Encoders

- The **variational lower bound** on the log-likelihood is given by

$$\log p_{\theta}(x|z) \geq E_{q_{\theta}}[\log p_{\theta}(x|z)] - D_{KL}(q_{\varphi}(z|x)||p_{\theta}(z))$$

- $q_{\varphi}(z|x)$ is an approximation of $p_{\theta}(z|x)$, parameterised by a neural network (**the encoder**). Typically $N(\mu(x), \sigma^2(x))$.
- In maximising the variational lower bound, the encoder and decoder are trained simultaneously.
- We use the decoder mean to define ϕ , i.e., $\mathbf{x} = \mu_{\mathbf{x}}(z)$.



Bayesian computation

- To compute probabilities and expectations for $z|y$ we use *a preconditioned Crank Nicolson algorithm*, which is a slow but robust Metropolized MCMC algorithm.
- For additional robustness w.r.t. multimodality, we run $M+1$ parallel Markov chains targeting $p(z)$, $p^{\frac{1}{M}}(z|y)$, $p^{\frac{2}{M}}(z|y)$, ..., $p(z|y)$, and perform randomized chain swaps.
- Probabilities and expectations for $x|y$ are directly available by ϕ -pushing samples.
- We are developing fast gradient-based stochastic algorithms. Naïve off-the-shelf implementations are not robust and have poor theoretical guarantees in this setting.

Previous works

- Our work is closely related to the Joint MAP method of M. González et al. (2019) arXiv:1911.06379, which considers a similar setup but seeks to compute the maximiser of $p(x, z|y)$ by alternating optimization.
- It is also related to works that seek to learn $p\left(x|y, \{x'_i\}_{i=1}^M\right)$ by using a GAN, e.g., Adler J et al. (2018) arXiv:1811.05910 and Zhang C et al. (2019) arXiv:1908.01010.
- More generally, part of a literature on data-driven regularization schemes; see Arridge S, Maass P, Oktem O, and Schönlieb CB (2019) Acta Numerica, 28:1-174.
- Underlying vision of Bayesian imaging methodology set in the seminal paper Besag J, Green P, Higdon D, Mengersen K (1995) Statist. Sci., 10 (1), 3--41.

Outline

- Introduction
- Proposed method
- **Experiments**

Experiments

- We illustrate the proposed approach with three imaging problems: denoising, deblurring (Gaussian blur 6x6 pixels), and inpainting (75% of missing pixels).
- For simplicity, we used the MNIST dataset (training set 60,000 images, test set 10,000 images, images of size 28x28 pixels). In our experiments we use approx. 10^5 iterations and 10 parallel chains. Computing times of the order of 5 minutes.
- We report comparisons with J-MAP of Gonzales et al. (2019) and plug-and-play ADMM of Venkatakrishnan (2013) using a deep denoiser specialised for MNIST.

Dimension of the latent space

- The dimension of the latent space plays an important role in the regularization of the inverse problem and strongly impacts the quality of the model.
- We can easily identify suitable dimensions by looking at the empirical marginal $p(z)$ obtained from encoded training examples, e.g., we look at the trace of $\text{cov}(z)$.

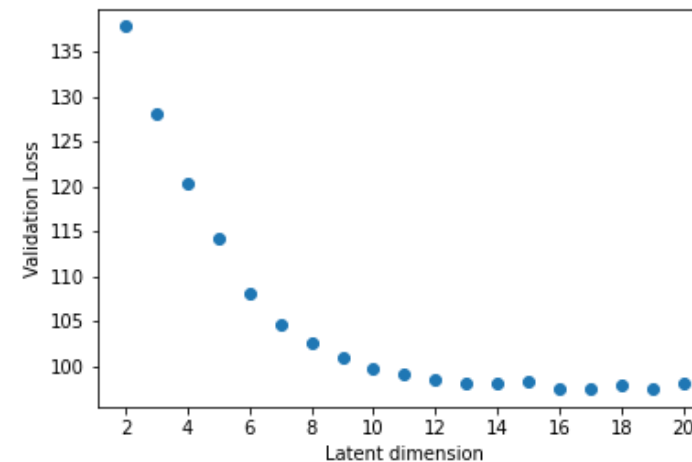
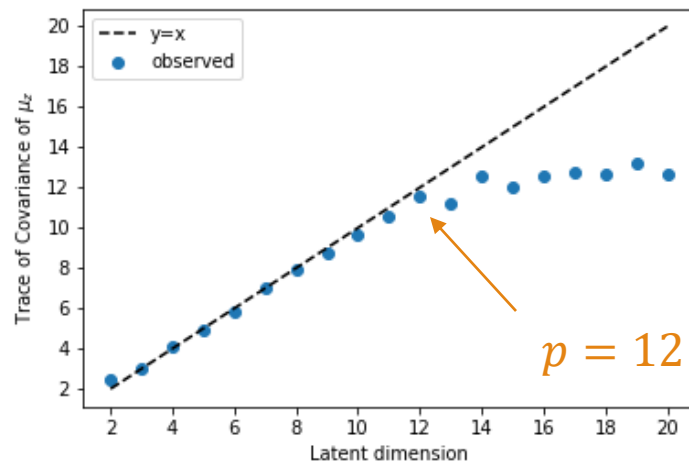
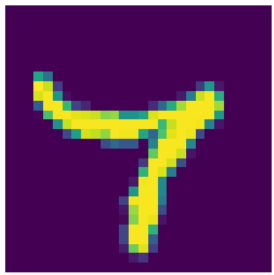


Image denoising

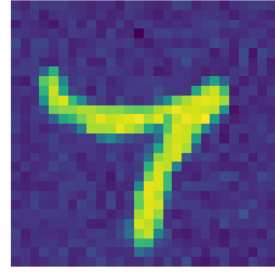
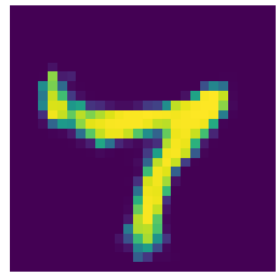
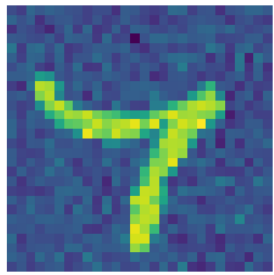
$\phi(E(z|y))$

Joint-MAP

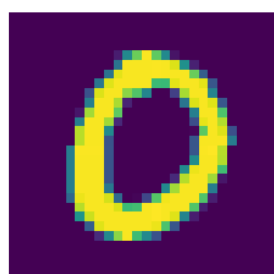
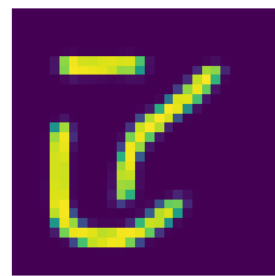
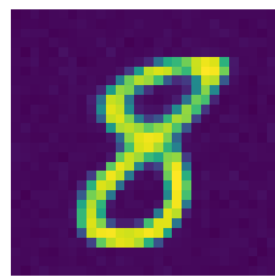
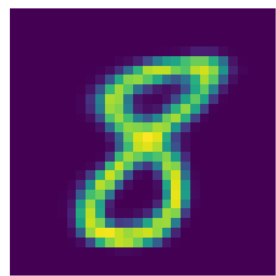
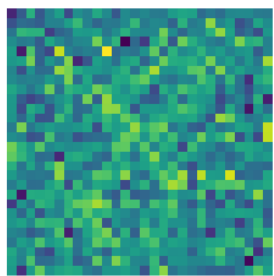
Plug-n-Play
ADMM



PSRN 20 dB



PSRN 0.5 dB



PSRN -8 dB

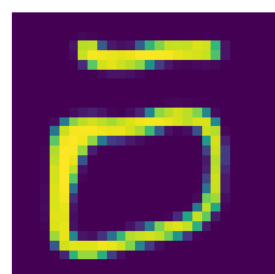
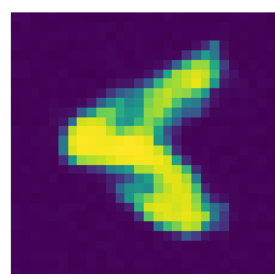
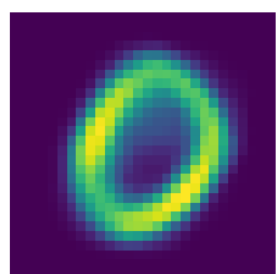
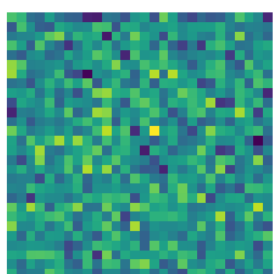
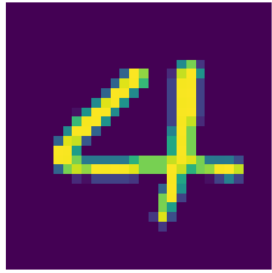


Image deblurring

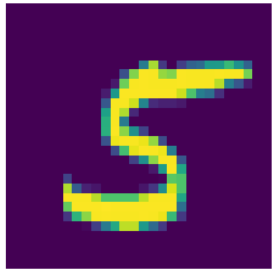
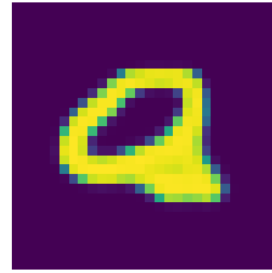
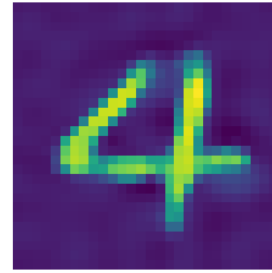
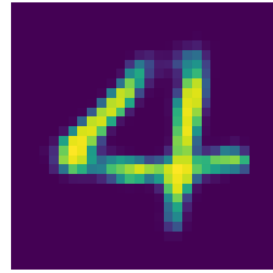
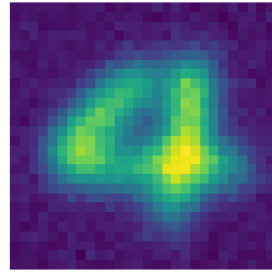
$\phi(E(z|y))$

Joint-MAP

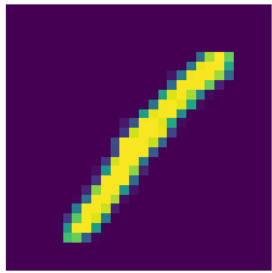
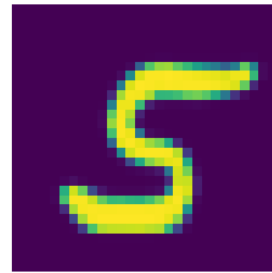
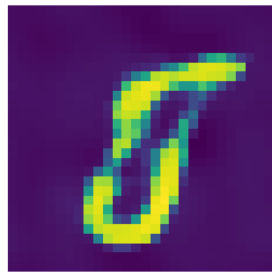
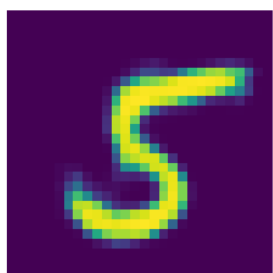
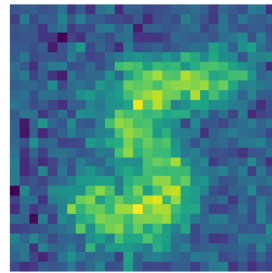
Plug-n-Play
ADMM



BSRN 32 dB



BSRN 20 dB



BSRN 12 dB

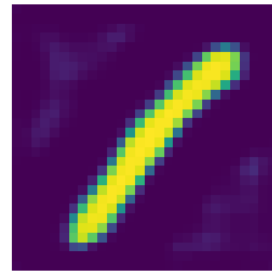
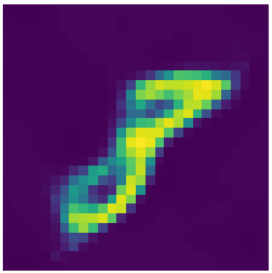
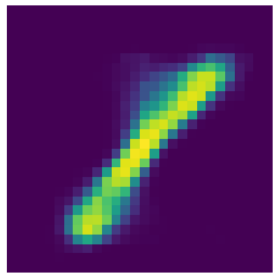
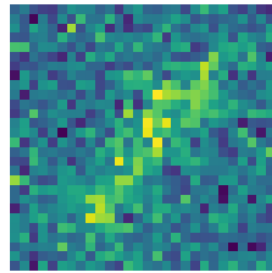


Image inpainting

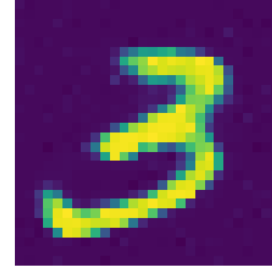
$\phi(E(z|y))$

Joint-MAP

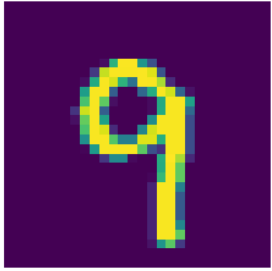
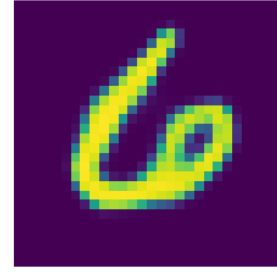
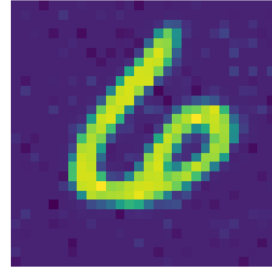
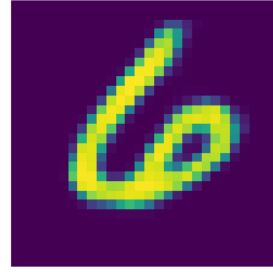
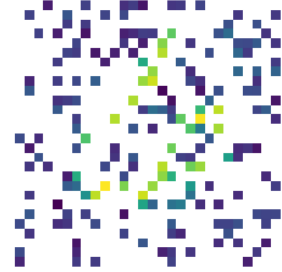
Plug-n-Play
ADMM



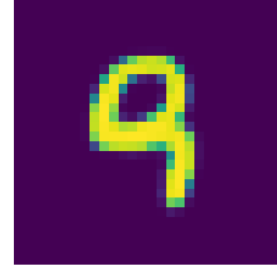
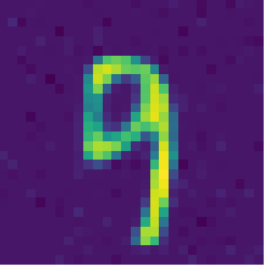
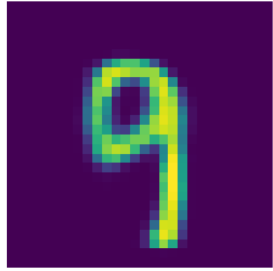
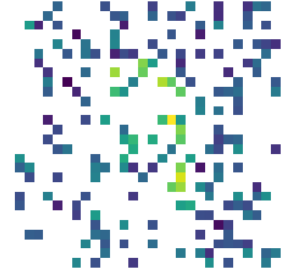
PSRN 37 dB



PSRN 25 dB



PSRN 18 dB

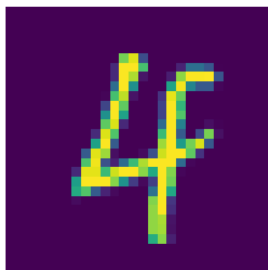


Uncertainty visualization

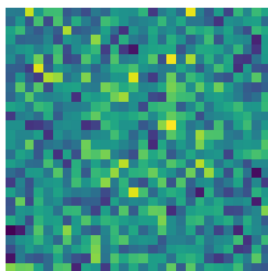
- Inverse problems that are ill-conditioned or ill-posed typically have high levels of intrinsic uncertainty, which are not captured by point estimators.
- As a way of visualizing this uncertainty, we compute an eigenvalue decomposition of the (latent) posterior covariance matrix to identify its two leading eigenvectors.
- We then produce a **grid of solutions** across this two-dimensional subspace.

Visualizing uncertainty

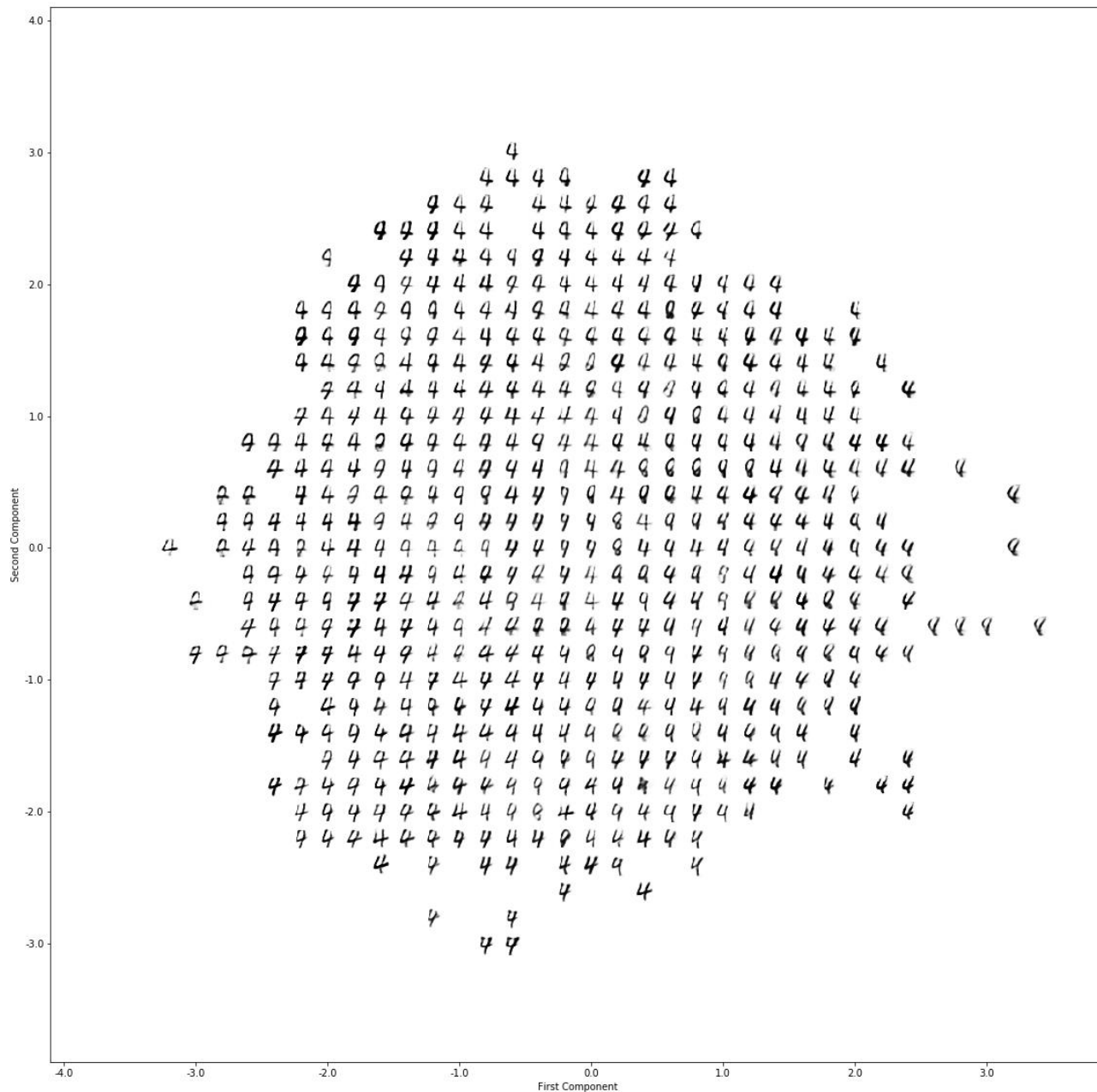
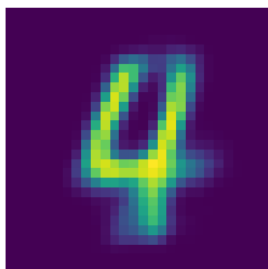
Truth



Noisy
Observation

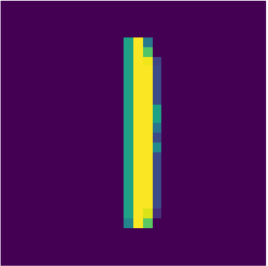


$\phi(E(z|y))$

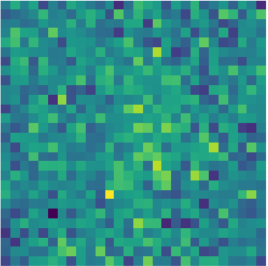


Visualizing uncertainty

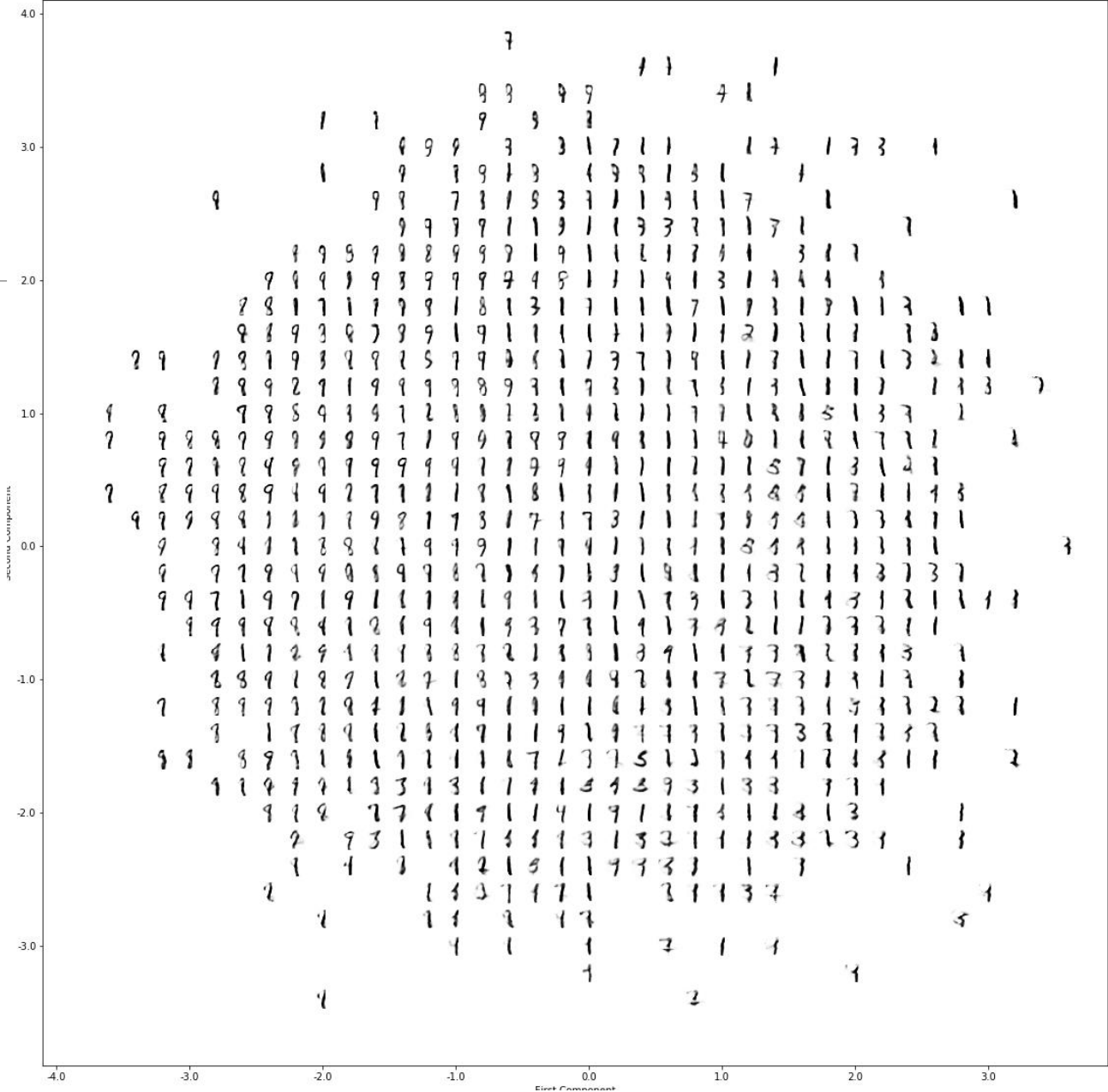
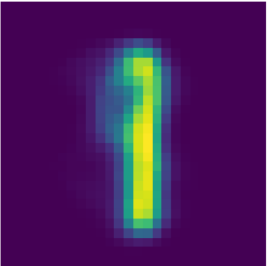
Truth



Blurred & Noisy Observation



$\phi(E(z|y))$



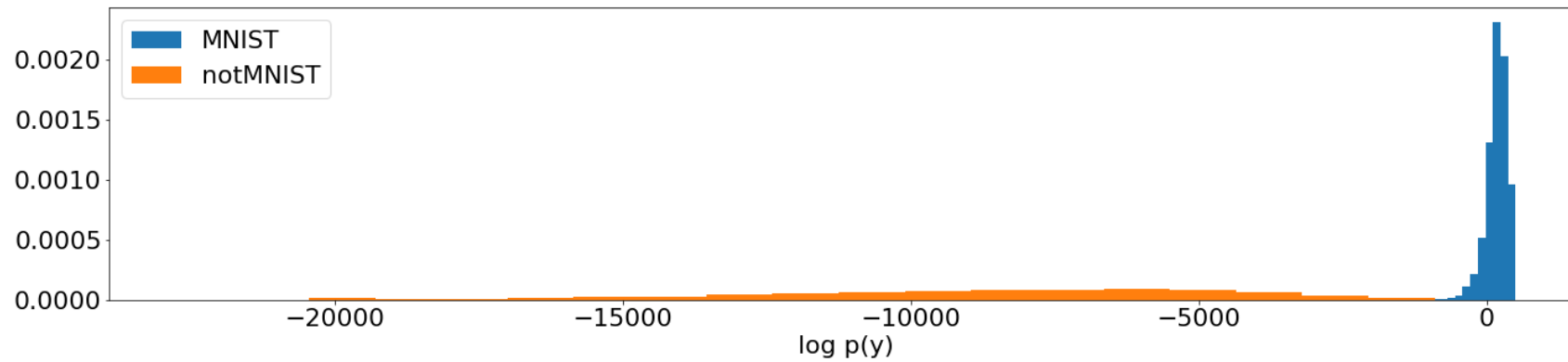
Warning of severe model misspecification

- Data-driven priors strongly concentrate probability mass in specific regions of the solution space.
- When used appropriately, then can deliver impressive results.
- However, **data-driven priors easily override the likelihood** and can lead to severe model misspecification when the truth differs significantly from the training examples.

Model misspecification testing

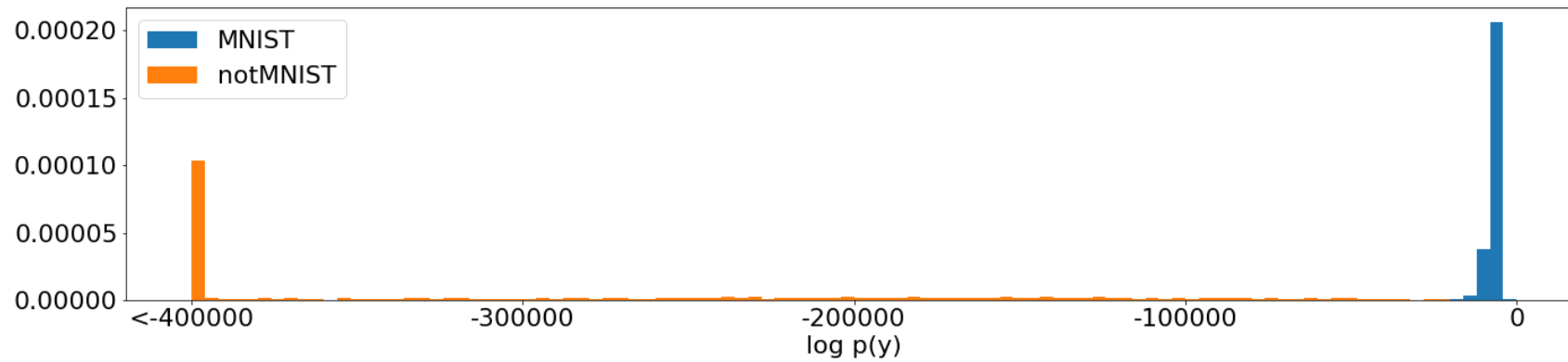
- When using data-driven priors it is important to perform model misspecification diagnosis tests.
- In the spirit of the Neyman-Pearson Lemma, we construct a statistical test based on the marginal likelihood $p(y)$ that we estimate from the chains.
- We compute this statistic for synthetic observations generated from the training dataset to establish the null distribution.
- This then allows misspecification testing and reporting p-values for observed data.

Model misspecification test



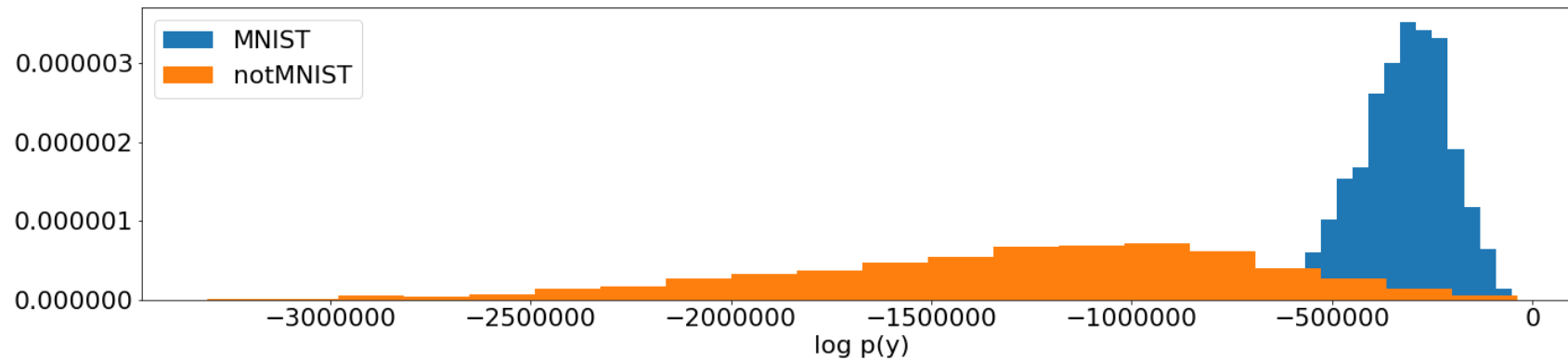
Denoising experiment ($\sigma = 0.1$). Reject null hypothesis (MNIST) with 99% confidence, and **average power of 99.6% for NotMNIST dataset.**

Model misspecification test



Deblurring experiment ($\sigma = 0.01$). Reject null hypothesis (MNIST) with 99% confidence, and **average power of 99.8%** for `NotMNIST` dataset.

Model misspecification test

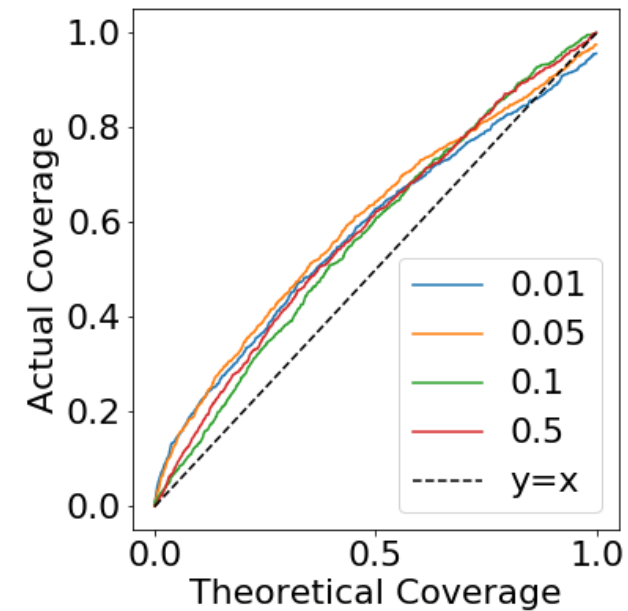
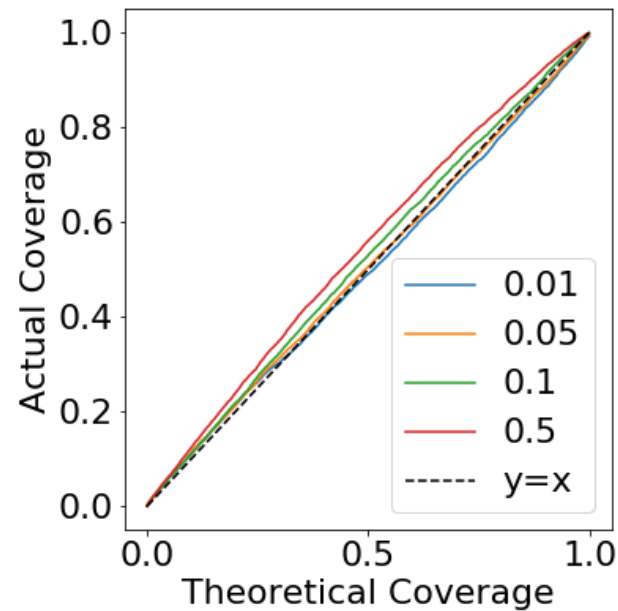


Inpainting experiment ($\sigma = 0.01$). Reject null hypothesis (MNIST) with 99% confidence, and **average power of 88.5%** for `NotMNIST` dataset.

Frequentist coverage of Bayesian probabilities

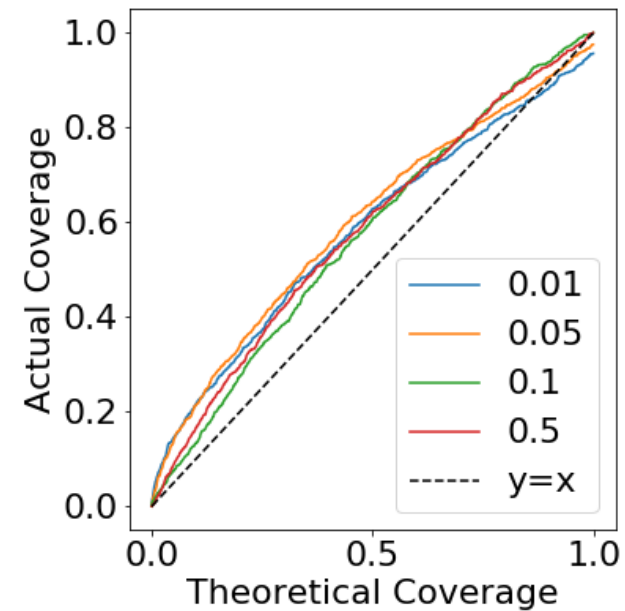
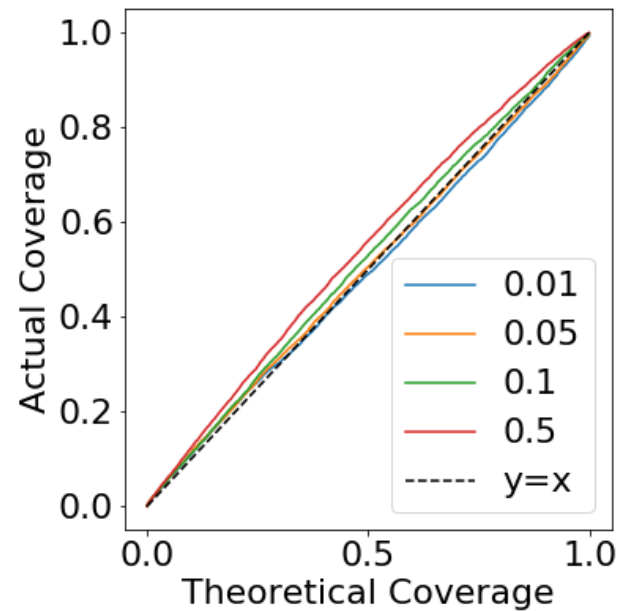
- Are the Bayesian probabilities reported by our models accurate in a frequentist sense? i.e., are they in agreement with empirical averages from repeated experiments?
- We explore this question by repeating experiments with 1,000 test images and measuring the empirical probabilities that the truth is within the $(1-\alpha)\%$ highest posterior density credible region.

Frequentist coverage of Bayesian probabilities



Coverage properties for denoising (left) and inpainting (right) for different noise levels (pixel dynamic range $[0, 1]$).

Frequentist coverage of Bayesian probabilities



To the best of our knowledge, this is the first example of a Bayesian model with accurate frequentist coverage properties in an imaging setting, albeit with a very simple image dataset!



Thank you!